Abnormal Fibrillin Assembly by Dermal Fibroblasts from Two Patients with Marfan Syndrome

Cay M. Kielty and C. Adrian Shuttleworth

School of Biological Sciences, University of Manchester, Medical School, Manchester M13 9PT, United Kingdom

Abstract. The microfibrillar glycoprotein fibrillin is linked to the Marfan syndrome, an autosomal dominant connective tissue disorder. In this study, fibrillin synthesis, deposition and assembly has been investigated in Marfan dermal fibroblast lines from two unrelated patients for whom distinct mutations in the fibrillin gene *FBN1* have been identified. In patient NB, a point mutation has occurred which causes an amino acid substitution and the other patient (GK) has a deletion in one allele.

The two cell lines were broadly comparable with respect to de novo fibrillin synthesis and its distribution between medium and cell layer compartments. Electrophoresis of fibrillin immunoprecipitates confirmed the presence of fibrillin in medium and cell layers. GK cells secreted an additional higher relative molecular mass fibrillin-immunoreactive component. The time-course of fibrillin secretion was similar for the two lines, but differences in fibrillin aggregation were apparent.

Rotary shadowing electron microscopy of extracted cell layers demonstrated the presence of abundant and extensive microfibrils in NB cell layers. These were abnormal in their gross morphology in comparison to microfibrils isolated from control cultures. No periodic microfibrillar structures were isolated from GK cell layers.

These studies underline the need to classify fibrillin defects in terms of biochemical and ultrastructural criteria. Examination of the effects of individual mutations on microfibril organization will be particularly informative in elucidating the relationship between microfibril dysfunction and the complex clinical manifestations of Marfan patients.

It is now well established that mutations in the fibrillin gene (*FBN1*) on chromosome 15 are the primary lesions in the heritable connective tissue disorder, Marfan syndrome, which is characterized by cardiovascular, skeletal, and ocular abnormalities (Dietz et al., 1991, 1992*a*,*b*; 1993*a*,*b*; Kainulainen et al., 1991, 1992, 1993; Lee et al., 1991; Godfrey et al., 1993; Hewitt et al., 1993). The glycoprotein fibrillin is a major structural component of a distinct class of extracellular matrix microfibrils which are key determinants of connective tissue architecture and integrity (Sakai et al., 1986, 1991). The fibrillin-containing microfibrils have a widespread tissue distribution and are particularly abundant in elastic tissues such as aorta, ligament, and skin where they are components of elastic fibers which generate elastic recoil (Cleary and Gibson, 1983). Ultrastructurally indistinguishable microfibrils are present in many non-elastic tissues such as the ocular zonule, tendon, and bone where they may serve an anchoring function (Fleischmajer et al., 1991; Keene et al., 1991*a*,*b*). These microfibrils have a complex ultrastructure with a diameter of 10–14 nm and an average, but variable, beaded periodicity of 50–55 nm (Fleischmajer et al., 1991; Keene et al., 1991*b*; Kielty et al., 1991, 1993*a*).

The recent cloning and sequencing of fibrillin has revealed that this protein contains a complex multi-domain structure (Maslen et al., 1991; Corson et al., 1993; Pereira et al., 1993). The molecule comprises multiple epidermal growth factor (EGF)-like motifs interspersed with 8-cysteine repeats with homology to the TGF-β1 binding protein and several apparently unique cysteine-rich motifs. However, the organization of fibrillin monomers within assembled microfibrils and the molecular interactions involved in their polymerization are largely undefined. It has been suggested that fibrillin monomers associate in a head-to-tail arrangement which may be stabilized by inter-molecular disulphide bonds (Sakai et al., 1991). Furthermore, calcium-binding by EGF-like domains may profoundly influence microfibril assembly by stabilizing conformations required for protein–protein interactions or by forming bridges between domains (Handford et al., 1991).

The Marfan syndrome has an autosomal dominant inheritance pattern with virtually complete penetrance, but at the clinical level is characterized by a strikingly heterogeneous spectrum of inter- and intra-familial phenotypes (Godfrey, 1993). The complexity of this disorder is reflected by the

Address all correspondence to C. M. Kielty, School of Biological Sciences, University of Manchester, Medical School, Oxford Road, Manchester M13 9PT, UK.

range of fibrillin mutations which have now been identified (Dietz et al., 1991, 1992*a*,*b*, 1993*a*,*b*; Kainulainen et al., 1991, 1992, 1993; Lee et al., 1991; Godfrey et al., 1993; Hewitt et al., 1993). There are to date, however, no satisfactory molecular explanations for how distinct fibrillin mutations affect microfibril assembly and functionality.

To gain insights into Marfan genotype:phenotype relationships, we have used a combined biochemical and ultrastructural approach to investigate fibrillin expression and assembly in dermal fibroblasts from two unrelated Marfan patients with defined mutations. In one case, a T to A point mutation substitutes the first highly conserved aspartate for glutamate within the calcium-binding consensus sequence of an EGF-like motif (Kainulainen et al., 1993). This patient, from a moderately affected two generation family, has predominantly skeletal manifestations. In the other case, a deletion corresponding to an exon encoding an EGF-like motif has occurred in one allele (Godfrey et al., 1993). This mutation occurs in a four-generation family with skeletal, cardiovascular, and ocular involvement. Correlation of microfibrillar abnormalities with these mutations has contributed insights into the molecular basis of the Marfan syndrome.

Materials and Methods

Materials

Bacterial collagenase (type 1A), phenylmethanesulphonyl fluoride (PMSF), *N*-ethylmaleimide (NEM), Tween 20, and prestained molecular weight markers were obtained from Sigma Chemical Co. (Poole, Dorset, UK). CNBr-activated Sepharose CL-4B, Sepharose CL-2B, protein A–Sepharose, and molecular weight markers were supplied by Pharmacia-LKB (Milton Keynes, Bucks, UK). Tissue culture media and plastics were obtained from GIBCO BRL (Paisley, Scotland, UK). The radioisotope [^{35}S]-TranSlabel was obtained from ICN Biomedicals Ltd. (High Wycombe, Bucks, UK). Marfan dermal fibroblast cell lines established from skin biopsies were used in these investigations. The cell line NB was supplied by Dr. Anne H. Child (St George's Hospital Medical School, London, UK) and Dr. F. Michael Pope (MRC Clinical Research Centre, Northwick Park Hospital, London, UK), and the cell line GK by Dr. Maurice Godfrey (Hollister Research Laboratories, Omaha, NE).

Cells and Cell Culture

Marfan and control dermal fibroblasts were routinely maintained in Dulbecco's minimum essential medium supplemented with 10% foetal calf serum, penicillin (400 U/ml), streptomycin (50 mg/ml), and glutamine (200 mg/ml). Confluent cells were labeled for 18 h with [^{35}S]TranSlabel in medium containing 0.5% foetal calf serum. In some experiments, cells were pulse labeled for 30 min with 250 μCi label, then chased for 1, 2, 6, and 24 h. Labeled medium was fractionated by addition of solid $(NH_4)_2SO_4$ to 30% saturation at 4°C in the presence of 5 mM NEM, 2 mM PMSF, and 10 mM EDTA. Cell layers were sequentially extracted in 0.05 M Tris/HCl, pH 7.4, containing 0.4 M NaCl, 0.005 M EDTA, and 1% (vol/vol) Nonidet P40 (NET buffer), and 0.05 M Tris/HCl, pH 7.4, containing 4.0 M guanidine HCl ($GuCl_2$). Extracts were clarified by centrifugation for 15 min at 7,500 *g* on a bench microfuge, and soluble supernatants retained for analysis.

For microfibril extractions, cells were maintained at post-confluence for up to three weeks. Cell layers were washed in 0.05 M Tris/HCl, pH 7.4, containing 0.4 M NaCl, then incubated for 3 h at 20°C in 0.05 M Tris/HCl, pH 7.4, containing 0.4 M NaCl, 0.005 M $CaCl_2$, 0.1 mg/ml bacterial collagenase (type 1A), 2 mM PMSF, and 5 mM NEM. Soluble extracts were clarified by centrifugation for 15 min at 7,500 *g* on a bench microfuge before size fractionation by gel filtration chromatography.

Size Fractionation of Fibrillin Solubilized from Cell Layer Extracts

Metabolically labeled GK and NB cell layer $GuCl_2$ extracts from 2 and 6 h pulse-chase time points were chromatographed on an analytical gel filtration column (1.5 × 25 cm) of Sepharose CL-2B. The column was equilibrated and eluted at room temperature with 0.05 M Tris/HCl, pH 7.4, containing 4.0 M $GuCl_2$. In each run, 60 × 1 ml fractions were collected. The elution positions of newly synthesized, metabolically labeled fibrillin were determined by immunoprecipitating fibrillin from appropriately pooled fractions.

Postconfluent cell layer extracts solubilized by bacterial collagenase digestion were chromatographed directly without concentration under non-reducing, nondenaturing conditions on a Sepharose CL-2B column equilibrated and eluted at room temperature with 0.05 M Tris/HCl, pH 7.4, containing 0.4 M NaCl. High-M_r material present in the excluded volume (Vo) was retained for ultrastructural analysis.

Immunoprecipitation

Immunoprecipitation was carried out in NET buffer as described by Kielty et al. (1990). Briefly, 30% $(NH_4)_2SO_4$ precipitates of cell culture medium were taken up in 1 ml NET buffer. Cell layers were sequentially extracted with NET buffer and with 4.0 M $GuCl_2$. Cell layer $GuCl_2$ extracts were dialyzed extensively against 0.05 M Tris/HCl, pH 7.4, containing 0.4 M NaCl and 0.005 M EDTA, and 0.1% (vol/vol) Nonidet P40 was added before immunoprecipitation.

In view of the similar electrophoretic mobilities on SDS-PAGE of fibronectin and fibrillin, fibronectin was removed before immunoprecipitation of fibrillin by two sequential incubations with 100 μl 1:1 (vol/vol) solution of gelatin–Sepharose. Samples were then incubated for 1 h at 20°C with a 1:100 dilution of a polyclonal fibrillin antiserum (Shuttleworth et al., 1992; Kielty and Shuttleworth, 1993*a*; Waggett et al., 1993), before the addition of 60 ml of a 1:1 (vol/vol) solution of protein A–Sepharose in NET buffer.

Electrophoresis

Immunoprecipitates were separated by discontinuous SDS-PAGE on 6% gels (Laemmli, 1970) under non-reducing conditions, then analyzed by fluorography. Molecular weights were determined by reference both to prestained standards (fumarase [56,000], pyruvate kinase [65,000], fructose-6-phosphate kinase [88,000], β-galactosidase [125,000], α2 macroglobulin [190,000]) and unstained standards (bovine serum albumin [67,000], lactate dehydrogenase [140,000], catalase [232,000], ferritin [440,000], thyroglobulin [669,000]).

Ultrastructural Analysis

Void volume fractions of cell layer extracts were visualized for their microfibril content by rotary shadowing using a modification of the mica sandwich technique (Kielty et al., 1993). Immunogold electron microscopy was carried out as described by Waggett et al. (1993).

Results

Two Marfan dermal fibroblast lines were used in these investigations. NB cells have a T to A point mutation within FBN1 causing an aspartate to glutamate amino acid substitution (D1229E; Pereira et al., 1993) (Kainulainen et al., 1993). GK cells have an FBN1 allele with exon 54 (Pereira et al., 1993) deleted; this exon encodes a single EGF-like motif (Godfrey et al., 1993).

Count Distribution of Newly Synthesized Fibrillin

Metabolically labeled fibrillin was immunoprecipitated from medium and cell layer fractions after 18 h labeling. De novo fibrillin synthesis was expressed as total counts incorporated into fibrillin (Table I). The two lines synthesized comparable levels of fibrillin and in both cases the majority of newly synthesized fibrillin was deposited within the cell layer.

Pulse-Chase Labeling and SDS-PAGE Analysis of Fibrillin Immunoprecipitates

The electrophoretic mobility and time-course of secretion of

Table I. Distribution of Counts Incorporated into Fibrillin by Dermal Fibroblasts from Two Marfan Patients

Cell line	Medium		Cell layers		Total fibrillin counts
	cpm/1 × 10⁶ cells	%	*cpm/1 × 10⁶ cells*	%	
NB	3781	37	6435	63	10216
GK	1047	12	7678	88	8725

Cells were labeled for 18 h with [^{35}S]cysteine. Fibrillin was immunoprecipitated from 30% $(NH_4)_2SO_4$ precipitates of cell culture medium and from sequential detergent (NET) and denaturing ($GuCl_2$) cell layer extracts. The amount and distribution of newly synthesized fibrillin in the different cell cultures was compared by determining the total immunoprecipitable fibrillin counts in the medium and cell layer extracts. The figures represent a single experiment, but similar results were obtained in duplicate labeling experiments.

fibrillin into the medium by NB and GK cells was determined in pulse-chase experiments (Fig. 1). Metabolically labeled fibrillin was immunoprecipitated from medium after chase times of 30 min, 1, 2, 6, and 24 h, and analyzed on SDS-PAGE gels under non-reducing conditions. Under these conditions, fibrillin migrated as a single component (300 kD) with a similar electrophoretic mobility to that previously demonstrated for a range of normal cells (Kielty and Shuttleworth, 1993*a*). In the case of GK, a second higher relative molecular mass fibrillin-immunoreactive component (330 kD) was also present.

Labeled fibrillin was first detected in the medium of both cell lines after 2 h chase and in abundance by 6 h (Fig. 1 *A*). In the case of NB, there was evidence by 6 h for the formation of higher relative molecular mass disulphide-bonded intermediate assemblies and larger aggregates. Aggregation was also a feature of the fibrillin secreted by the line GK, since the majority of immunoreactive material did not enter the gel. Further, a 330-kD fibrillin-immunoreactive component present in GK medium was seen to accumulate over a 24-h period. The time-course of secretion of this component appeared similar to fibrillin but its subsequent fate was quite distinct, and if it is being incorporated into aggregates this process must be occurring at a much reduced rate.

A more complex electrophoretic pattern was observed for fibrillin immunoprecipitated from cell layer $GuCl_2$ extracts (Fig. 1 *B*). In the case of GK, a component of 330 kD, a doublet migrating around 300 kD and a lower relative molecular mass doublet (270 kD) were detected. In contrast, newly synthesised fibrillin in NB cell layer extracts was immunoprecipitated as high relative molecular mass aggregates.

Size Fractionation of Cell Layer Extracts

Aggregation of newly synthesized fibrillin within the $GuCl_2$-soluble cell layer compartments of NB was also demonstrated by size fractionation of metabolically labeled fibrillin (Fig. 2). There was a clear shift in the elution profile of labeled fibrillin between 2 and 6 h indicating increasing molecular mass (Fig. 2 *B*). No comparable change in elution pattern was detected between 2 and 6 h in GK cell layer extracts.

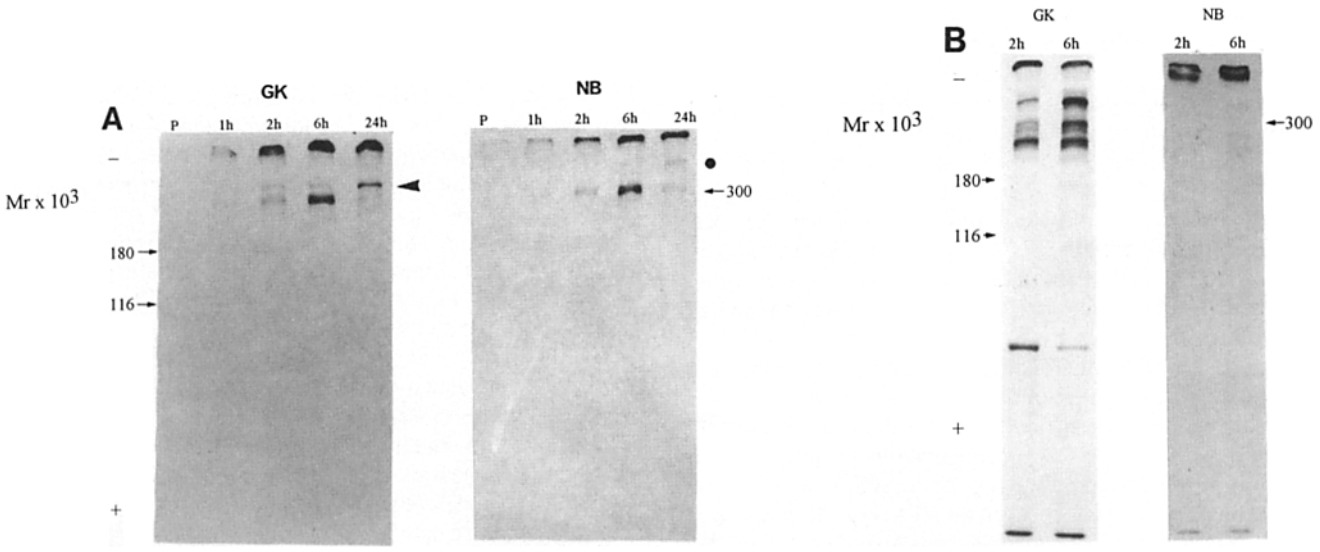

Figure 1. Pulse-chase metabolic labeling and analysis of newly synthesized fibrillin by SDS-PAGE. Cells were pulse-labeled with [^{35}S]TranSlabel for 30 min, then chased for 30 min, 1, 2, 6, and 24 h. Fibrillin immunoprecipitates from medium and cell layer fractions were analyzed by SDS-PAGE on 6% gels under non-reducing conditions, and fluorography. (*A*) Newly synthesized fibrillin secreted into medium. Medium was fractionated with $(NH_4)_2SO_4$ to 30% saturation in the presence of inhibitors before immunoprecipitation of fibrillin. Secreted fibrillin monomers (300 kD) and high relative molecular mass fibrillin-immunoreactive material which failed to enter the stacking gel were identified in the medium of GK and NB cells from 2 h. In the case of NB cells, an aggregate of intermediate electrophoretic mobility was also present (*black dot*). GK cells secreted an additional fibrillin-immunoreactive component (330 kD) which accumulated in the medium and did not appear to aggregate over 24 h (*large arrowhead*). (*B*) Newly synthesized fibrillin present in cell layers. Fibrillin was immunoprecipitated from $GuCl_2$-extracted cell layers at 2 and 6 h. GK cell layer extracts exhibited a complex pattern of fibrillin-immunoreactive bands, with a 330-KD component, a doublet (300 KD), a lower relative molecular mass doublet (270 kD) and another further band (55 kD). These components accumulated between 2 and 6 h, particularly the 330-kD band. Extracts of NB cell layers from 2 and 6 h of chase contained high relative molecular mass aggregates of fibrillin.

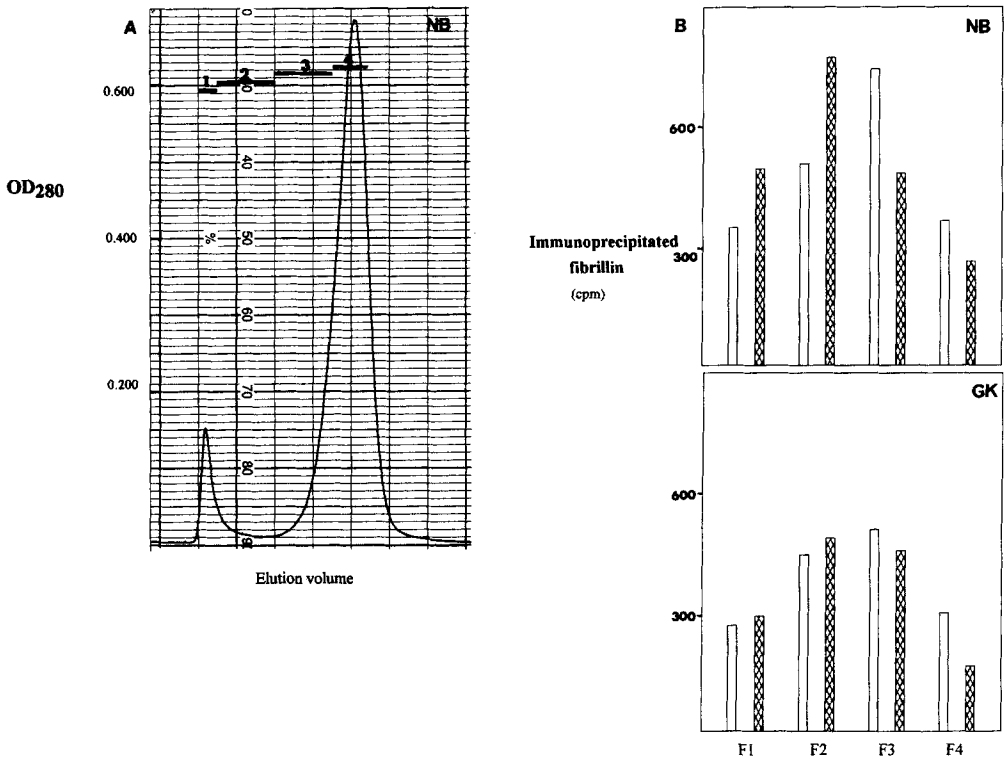

Figure 2. Time course of aggregation of newly synthesized fibrillin in cell layers. $GuCl_2$ cell layer extracts at 2 and 6 h chase time points were size fractionated by gel filtration chromatography on an analytical Sepharose CL-2B column (see Materials and Methods). The eluted volume was pooled into four fractions as indicated before fibrillin immunoprecipitation. Total fibrillin counts immunoprecipitated from pooled fractions of 2 and 6 h extracts were determined. (*A*) Chromatography profile of NB cell layer extract. The OD_{280} traces for GK cell layer extracts were similar. (*B*) Histograms showing total immunoprecipitated fibrillin counts in each pooled fraction at 2 h (*open bars*) and 6 h (*cross-hatched bars*).

Ultrastructural Analyses

Examination by rotary shadowing electron microscopy of high relative molecular mass material solubilized from post-confluent bacterial collagenase-solubilized cell layers demonstrated the presence of extensive and abundant microfibrils in control and NB cell layers (Fig. 3, *A* and *B*). The microfibrils elaborated by control fibroblasts were similar in morphology to those previously isolated from tissues (Kielty et al., 1991, 1993*a*). In marked contrast to the control cultures, the microfibrils extracted from NB cell layers were clearly abnormal in the interbead domains which were diffuse and poorly defined. This structural variation was apparent in all fields. In the case of GK cell layer extracts, no morphologically identifiable periodic microfibrillar assemblies were demonstrable.

The identity of the microfibrillar assemblies was confirmed using immunogold localization of fibrillin epitopes (Fig. 4). Microfibrils from control cultures and those elaborated by NB cells were recognized by anti-fibrillin serum. The NB microfibrils were markedly irregular in outline in comparison to those elaborated by normal cells (Fig. 4, *A* and *B*). Fibrillin-immunoreactive material was also detected in GK cell layer extracts (Fig. 4 *C*).

Discussion

After the recent cloning and sequencing of the fibrillin gene *FBN1* and its linkage to the Marfan syndrome, interest has focussed on documenting fibrillin mutations as a first step to defining genotype: phenotype relationships (Lee et al., 1991; Dietz et al., 1991, 1992*a*,*b*, 1993*a*,*b*; Godfrey et al., 1993; Hewitt et al., 1993; Kainulainen et al., 1991, 1992, 1993). Concurrently, efforts have been made to use biochemical assays to identify fibrillin defects manifest at the level of fibrillin synthesis, secretion, or deposition (McGookey-Milewicz et al., 1992; Raghunath et al., 1993). These methodologies, however, fail to address the central question concerning the structural and functional consequences of defined mutations, and as a consequence, the aetiology of Marfan syndrome and the molecular basis of the clinical heterogeneity characteristic of this disorder have to date eluded molecular definition. It is clear that characterization of microfibrillar abnormalities reflecting distinct mutations is essential in order to arrive at a comprehensive molecular explanation of the complex Marfan phenotype. The isolation of intact microfibrils from dermal fibroblast cultures has for the first time allowed direct correlation of biochemical defects and microfibrillar abnormalities with defined fibrillin mutations.

Examination by rotary shadowing electron microscopy of high relative molecular mass fractions material isolated from Marfan cell layers clearly showed that NB cells were capable of assembling abundant and extensive periodic microfibrils. However, the appearance of these microfibrils was abnormal with diffuse, poorly defined interbead domains, in sharp contrast to the structural organization apparent in microfibrils elaborated by normal fibroblasts. In even greater contrast, no morphologically identifiable microfibrils at all could be seen in GK cell layer extracts, although high molecular mass fibrillin assemblies were detected immunologically. These observations suggest that in both Marfan cell lines products of mutated alleles are secreted and become incorporated into fibrillin assemblies. This is the first direct visual evidence for abnormalities in fibrillin aggregation and in microfibrillar characteristics of Marfan patient cells. Studies have been described where attempts were made to classify Marfan cell lines in terms of defects in fibrillin secretion and deposition (McGookey-Milewitz et al., 1992). Those stud-

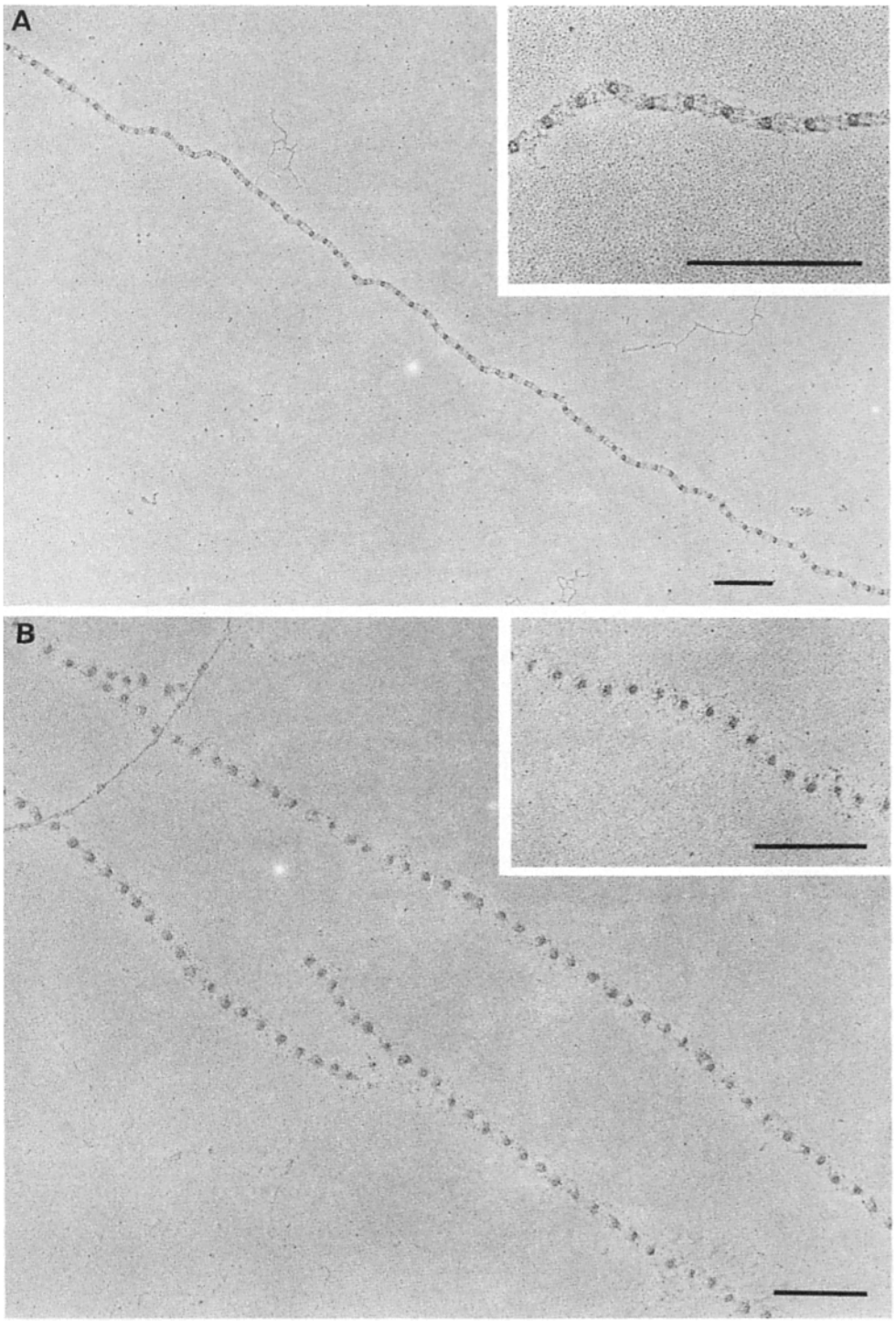

Figure 3. Electron micrographs after rotary shadowing of fibrillin-containing microfibrils isolated from postconfluent cell layers. Microfibrils were isolated from postconfluent cell layers of normal fibroblasts (*A*) and fibroblasts from patient NB (*B*). Fibrillin assemblies were clearly recognized by their distinctive beaded appearance. Microfibrils elaborated by the patient cells were morphologically distinct from those isolated from normal cultures, with ill-defined, diffuse interbead regions. The microfibrils shown were representative of all the fields examined for both cell types. Bars, 250 nm.

ies addressed the question of processing but not the aggregation of fibrillin. Here, we describe two Marfan dermal fibroblast lines for which the time-course of fibrillin secretion was similar to that previously described for a range of normal cells (Kielty and Shuttleworth, 1993*a*), but which exhibited differences with respect both to formation of aggregates in medium and cell layers and elaboration of a fibrillin-rich matrix. Some of these differences were manifest in the electrophoretic pattern of newly synthesized fibrillin secreted by the two lines. The major fibrillin band immunoprecipitated in both cases had a similar electrophoretic mobility (300 kD), which is surprising in view of the fact that the mutated FBN1 allele of GK encodes a polypeptide lacking 43 amino acids (Godfrey et al., 1993), but probably reflects the difficulties in resolving such large proteins electrophoretically. The identity of the 330-kD fibrillin-immunoreactive component secreted by GK cells is unclear and was not previously detected in fibrillin immunoprecipitates from normal cells

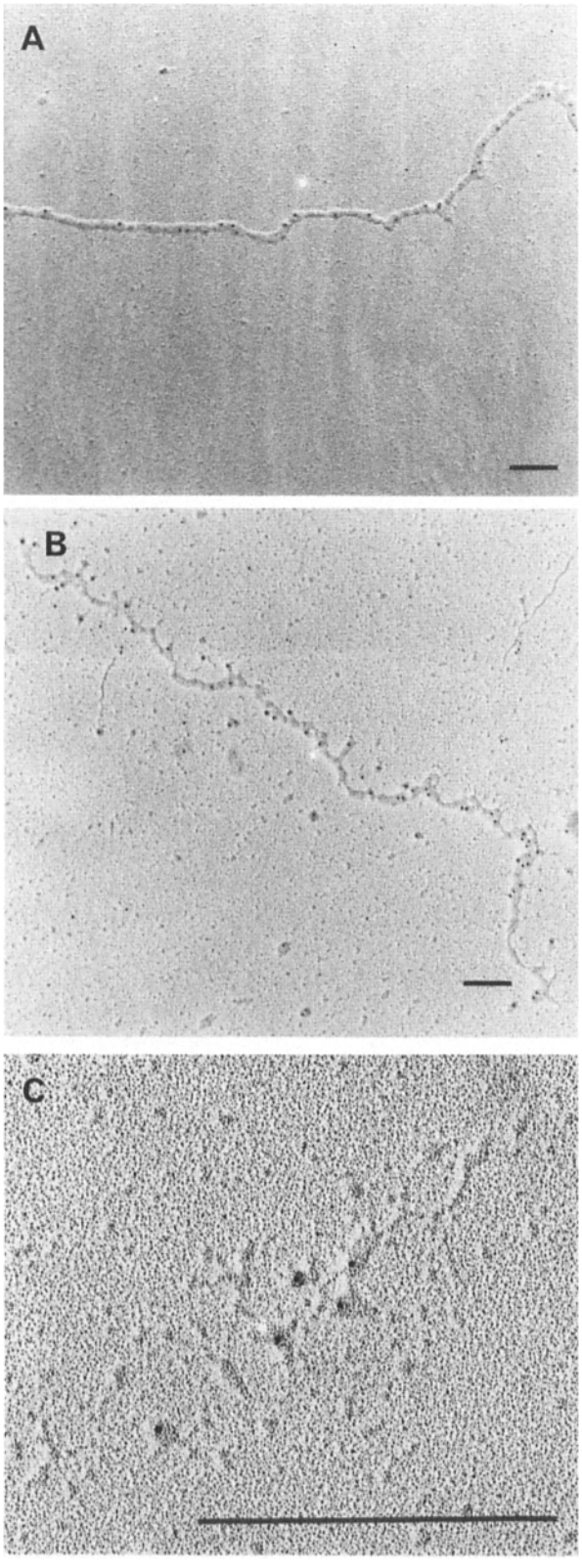

Figure 4. Electron micrographs after rotary shadowing of fibrillin assemblies treated with anti-fibrillin serum and second antibody-immunogold conjugate. Immunogold localization of fibrillin epitopes present on fibrillin assemblies isolated from normal fibroblasts (*A*), fibroblasts from patient NB (*B*), and fibroblasts from patient GK (*C*) confirmed the identity of the microfibrillar assemblies elaborated by normal and NB cells. The NB microfibrils were markedly irregular in outline in comparison to those elaborated by normal cells. Fibrillin-immunoreactive aggregates, but no microfibrils, were detected in GK cell layer extracts. Bars, 250 nm.

(Kielty and Shuttleworth, 1993*a*), although a component of similar size has been described in fibrillin immunoprecipitates from cell lysates (McGookey-Milewicz et al., 1992). If the component represents the product of a mutated allele, it is unclear whether it cannot be incorporated into microfibrils or whether it can be incorporated but at a much reduced rate. The failure to detect normal microfibrils however, implicates the product of the mutated allele in fibrillin polymerization. The presence of the 330-kD component might imply a processing defect although there is no consensus on the occurrence of fibrillin processing or its role in microfibril assembly. The existence of a precursor form of fibrillin has, however, been suggested from immunoprecipitation experiments where both fibrillin and "profibrillin" molecules larger than fibrillin by ~30,000 were identified (McGookey-Milewicz et al., 1993). In the case of NB, fibrillin aggregation to high relative molecular mass assemblies followed a similar pattern to that previously observed for normal cells (Kielty and Shuttleworth, 1993*a*), and this was reflected in their capacity to make microfibrils.

It is established that fibrillin is the major structural element of this class of connective tissue microfibrils (Sakai et al., 1986, 1991). However, it has recently been demonstrated that fibrillin exists as a family of isoforms encoded by distinct structural genes and a plethora of candidate microfibril-associated molecules including microfibril-associated glycoprotein (MAGP) have also been described (Gibson et al., 1991). The precise molecular composition of the microfibrils and their mechanism of assembly remain to be resolved. It is clear, however, from the present study that defective fibrillin encoded by the FBN1 locus has considerable influence on microfibrillar stability.

The exon deletion that occurs in GK is one of several deletion mutations that have been described in Marfan patients (Kainulainen et al., 1992, 1993; Dietz et al., 1993*a*; Godfrey et al., 1993). These deletions reflect distinct mutations within the *FBN1* gene. In one case, a genomic deletion spanning three EGF-like motifs has occurred (Kainulainen et al., 1992). An unusual exon-skipping mutation caused by a premature termination has also been described (Dietz et al., 1993*a*). Two examples of intronic mutations causing splicing defects and resulting in both cases in the skipping of an exon encoding an entire EGF-like domain, have been reported (Godfrey et al., 1993; Kainulainen et al., 1993). In the case of patient GK, the single exon deletion arises as a consequence of a donor splice site mutation (Godfrey et al., 1993). It remains to be seen whether the mechanism or position of the splice variants reflects the severity of the condition.

At a clinical level, the proband GK has major cardiovascular, skeletal, and ocular symptoms. The skeletal manifestations include excessive height, arachnodactyly, scoliosis, pectus excavatum, marked joint instability, and dolichostenomelia. In addition, echcardiography has revealed mitral valve prolapse and regurgitation and a dilated aortic root, and the patient also suffers from ectopia lentis and severe myopia (Godfrey et al., 1993). One explanation for the com-

prehensive structural disruption to the microfibrils in GK cultures is that shortened products of the mutated allele cannot align correctly to form the intermolecular interactions required to ensure microfibrillar integrity. In contrast, the patient NB is an affected member of a two-generation family with predominantly skeletal manifestations. The phenotype includes excessive height, kyphoscoliosis, hypermobile joints which dislocate, aortic dilatation, stretchy skin, easy bruisability, umbilical hernia, prematurity, and duodenal ulcer, but a lack of all ocular symptoms (Kainulainen et al., 1993). The single base change described for NB is one of a number of examples of point mutations in FBN1 that are linked to Marfan syndrome (Dietz et al., 1991, 1992*a*,*b*, 1993*b*; Kainulainen et al., 1993). In this case, the aspartate to glutamate amino acid substitution within the calcium-binding consensus sequence of an EGF-like domain is predicted to disrupt calcium-binding and monomer conformation (Kielty and Shuttleworth, 1993*b*). Our identification of abnormal microfibrils elaborated by NB cells supports this notion and suggests that the mutation itself may be located within the interbead domain. A fascinating feature of the extensive microfibrils elaborated by NB cells is that despite their disrupted organization, the periodicity remains remarkably constant.

Despite the number of mutations that have been reported, and the relationship that has been established between FBN1 and Marfan syndrome, no comprehensive molecular explanation of microfibril structure and function arising from these data has been derived to date. The approach outlined in this study provides a means to test structure: function predictions and how individual mutations give rise to the heterogeneous clinical manifestations of Marfan syndrome. We have described microfibrillar abnormalities characteristic of two patient cell lines which reflect the structural and functional disruptions that manifest in these patients as distinct clinical phenotypes. It is anticipated that further similar analyses of further patient lines with defined mutations will provide major insights into genotype: phenotype relationships of Marfan syndrome. The correlation of microfibrillar abnormalities with defined fibrillin mutations will also undoubtedly shed light on the complex process of microfibril assembly.

This work was supported by the Medical Research Council and Wellcome Trust.

Received for publication 15 October 1993, and in revised form 13 December 1993.

References

Cleary, E. G., and M. A. Gibson. 1983. Elastin-associated microfibrils and microfibrillar proteins. *Int. Rev. Connect. Tissue. Res.* 10:97–209.

Corson, G. M.., S. C. Chalberg, H. C. Dietz, N. L. Charbonneau, and L. Y. Sakai. 1993. Fibrillin binds calcium and is coded by cDNAs that reveal a multidomain structure and alternatively spliced exons at the 5′ end. *Genomics.* 17:476–484.

Dietz, H. C., G. R. Cutting, R. E. Pyeritz, C. L. Maslen, L. Y. Sakai, G. M. Corson, E. G. Puffenberger, A. Hamosh, E. J. Nanthakumar, S. M. Curristin, G. Stetten, D. A. Meyers, and C. A. Francomano. 1991. Marfan syndrome is caused by a recurrent *de novo* missense mutation in the fibrillin gene. *Nature (Lond.).* 352:337–339.

Dietz, H. C., R. E. Pyeritz, E. G. Puffenberger, R. J. Kendzior, G. M. Corson, C. L. Maslen, L. Y. Sakai, C. A. Francomano, and G. R. Cutting. 1992*a*. Marfan phenotype variability in a family segregating a missense mutation in the epidermal growth factor-like motif of the fibrillin gene. *J. Clin. Invest.* 89:1674–1680.

Dietz, H. C., J. M. Savaiva, R. E. Pyeritz, G. R. Cutting, and C. A. Francomano. 1992*b*. Clustering of fibrillin (FBN1) missense mutations in Marfan syndrome patients at cysteine residues in EGF-like domains. *Hum. Mutat.* 1:366–374.

Dietz, H. C., D. Valle, C. A. Francomano, R. J. Kendzior, R. E. Pyeritz, and G. R. Cutting. 1993*a*. The skipping of constitutive exons *in vivo* induced by nonsense mutations. *Science (Wash. DC).* 259:680–683.

Dietz, H. C., I. McIntosh, L. Y. Sakai, G. M. Corson, S. C. Chalberg, R. E. Pyeritz, and C. A. Francomano. 1993*b*. Four novel FBN1 mutations: Significance for mutant transcript level and EGF-like domain calcium binding in the pathogenesis of Marfan syndrome. *Genomics.* 17:468–475.

Fleischmajer, R., J. S. Perlish, and T. Farraggiani. 1991. Rotary shadowing of collagen monomers, oligomers and fibrils during tendon fibrillogenesis. *J. Histochem. Cytochem.* 39:51–58.

Gibson, M. A., L. B. Sandberg, L. E. Grosso, and E. G. Cleary. 1991. Complementary DNA cloning establishes microfibril-associated glycoprotein to be a discrete component of the elastin-associated microfibrils. 266:7596–7601.

Godfrey, M. 1993. Molecular heterogeneity: a clinical dilemma. Clinical heterogeneity: a molecular dilemma. *Am. J. Hum. Genet.* 53:22–25.

Godfrey, M., N. Vandemark, M. Wang, M. Vellnov, D. Wargowskl, S. Droste, and V. H. Rao. 1993. Prenatal diagnosis and a donor splice site mutation in fibrillin in a family with Marfan syndrome. *Am. J. Hum. Genet.* 53:472–480.

Handford, P. A., M. Mayhew, M. Baron, P. R. Winship, I. D. Campbell, and G. G. Brownlee. 1991. Key residues involved in calcium-binding motifs in EGF-like domains. *Nature (Lond.).* 351:164–167.

Hewitt, D. R., J. R. Lynch, R. Smith, and B. Sykes. 1993. A novel fibrillin mutation in the Marfan syndrome which could disrupt calcium binding of the epidermal growth factor-like module. *Hum. Mol. Genet.* 2:475–477.

Kainulainen, K., B. Steinmann, F. Collins, H. C. Dietz, C. A. Francomano, A. H. Child, M. W. Kilpatrick, and L. Peltonen. 1991. Marfan syndrome: no evidence for heterogeneity in different populations, and more precise mapping of the gene. *Am. J. Hum. Genet.* 49:662–667.

Kainulainen, K., L. Y. Sakai, A. Child, F. M. Pope, L. Puhakka, L. Ryhanen, A. Palotie, I. Kaitila, and L. Peltonen. 1992. Two mutations in Marfan syndrome resulting in truncated fibrillin polypeptides. *Proc. Natl. Acad. Sci. USA.* 89:5917–5921.

Kainulainen, K., L. Karttunen, L. Puhakka, L. Y. Sakai, and L. Peltonen. 1994. Ten novel mutations of the FBN1 resulting in a wide variety of clinical phenotypes. *Nature (Genetics).* In press.

Keene, D. R., L. Y. Sakai, and R. E. Burgeson. 1991*a*. Human bone contains type III collagen, type VI collagen and fibrillin: type III collagen is present on specific fibers that may mediate attachment of tendons, ligaments and periosteum to calcified bone matrix. *J. Histochem. Cytochem.* 39:59–69.

Keene, D. R., B. K. Maddox, H.-J. Kuo, L. Y. Sakai, and R. W. Glanville. 1991*b*. Extraction of beaded structures and their identification as fibrillin-containing matrix microfibrils. *J. Histochem. Cytochem.* 39:441–449.

Kielty, C. M., and C. A. Shuttleworth. 1993*a*. Synthesis and assembly of fibrillin by fibroblasts and smooth muscle cells. *J. Cell Sci.* 106:167–173.

Kielty, C. M., and C. A. Shuttleworth. 1993*b*. The role of calcium in the assembly of fibrillin microfibrils. *FEBS (Fed. Eur. Biochem. Soc.). Lett.* 336:323–326.

Kielty, C. M., R. P. Boot-Handford, S. Ayad, C. A. Shuttleworth, and M. E. Grant. 1990. Molecular composition of type VI collagen. *Biochem. J.* 272: 787–795.

Kielty, C. M., C. Cummings, S. P. Whittaker, C. A. Shuttleworth, and M. E. Grant. 1991. Isolation and ultrastructural analysis of microfibrillar structures from bovine elastic tissues. *J. Cell Sci.* 99:797–807.

Kielty, C. M., L. Berry, S. P. Whittaker, and C. A. Shuttleworth. 1993. Microfibrillar assemblies of foetal bovine skin. Developmental distribution and relative abundance of type VI collagen and fibrillin. *Matrix.* 13:103–112.

Laemmli, U. K. 1970. Cleavage of structural proteins during assembly of the head of bacteriophage T4. *Nature (Lond.).* 227:680–685.

Lee, B., M. Godfrey, E. Vitale, H. Hori, M.-G. Mattei, M. Sarfarazi, P. Tsipouras, F. Ramirez, and D. W. Hollister. 1991. Linkage of Marfan syndrome and a phenotypically related disorder to two different fibrillin genes. *Nature (Lond.).* 352:330–334.

Maslen, C. L., G. M. Corson, B. K. Maddox, R. W. Glanville, and L. Y. Sakai. 1991. Partial sequence of a candidate gene for Marfan syndrome. *Nature (Lond.).* 352:334–337.

McGookey-Milewicz, D., R. E. Pyeritz, E. S. Crawford, and P. H. Byers. 1992. Marfan syndrome: defective synthesis, secretion, and extracellular matrix formation of fibrillin by cultured dermal fibroblasts. *J. Clin. Invest.* 89:79–86.

Pereira, L., M. D'Alessio, F. Ramirez, J. R. Lynch, B. Sykes, T. Pangilinan, and J. Bonadio. 1993. Genomic organization of the coding sequence for fibrillin, the defective gene product of Marfan syndrome. *Hum. Molec. Genet.* 2:961–968.

Pyeritz, R. E. The Marfan Syndrome. 1993. *In* Connective Tissue and Its Heritable Disorders, P. Royce and B. Steinmann, editors. Wiley-Liss, New York. 437–468.

Raghunath, M., A. Superti-Furga, M. Godfrey, and B. Steinmann. 1993. Decreased deposition of fibrillin and decorin in neonatal Marfan syndrome fibroblasts. *Hum. Genet.* 90:511–515.

Sakai, L. Y., D. R. Keene, and E. Engvall. 1986. Fibrillin, a new 350-kD glycoprotein is a component of extracellular microfibrils. *J. Cell Biol.* 103: 2499–2509.

Sakai, L. Y., D. R. Keene, R. W. Glanville, and H.-P. Bachinger. 1991. Purification and partial characterization of fibrillin, a cysteine-rich structural component of connective tissues. *J. Biol. Chem.* 266:14763–14770.

Shuttleworth, C. A., L. Berry, and C. M. Kielty. 1992. Microfibrillar elements in dental pulp: Presence of type VI collagen and fibrillin-containing microfibrils. *Arch. Oral Biol.* 37:1079–1084.

Tsipouras, P., R. Del Mastro, M. Sarfarazi, B. Lee, E. Vitale, A. H. Child, M. Godfrey, R. B. Devereux, D. Hewitt, B. Steinmann, D. Viljoen, B. C. Sykes, M. Kilpatrick, and F. Ramirez. 1992. Linkage analysis demonstrates that Marfan syndrome, dominant ectopia lentis, and congenital contractural arachnodactyly are linked to the fibrillin genes on chomosomes 15 and 5. *N. Engl. J. Med.* 326:905–909.

Waggett, A. D., C. M. Kielty, and C. A. Shuttleworth. 1993. Microfibrillar elements in the synovial joint: presence of type VI collagen and fibrillin-containing microfibrils. *Annu. Rheum. Dis.* 52:449–453.